J Nanostruct 16(3): 4234-4248, Summer 2026

RESEARCH PAPER

Multi Walled Carbon Nanotubes Incorporated Poly-Copper Phthalocyanine as Nano Composite Thin Films Deposited on Silicon-Silicon Dioxide Substrate for Photocurrent Efficiency

Baneen Jabar Abduljawad *, Hikmat Adnan Banimuslem

Department of Physics, College of Science, University of Babylon, Babylon, Iraq

ARTICLE INFO

Article History:
Received 08 April 2026
Accepted 12 June 2026
Published 01 July 2026

Keywords:
Carbon nanotube
DC conductivity
Nanostructure
Phthalocyanine
Photocurrent

ABSTRACT

An interaction was observed, and to explore its effect on optical, electrical, and photoelectric properties, we prepared a hybrid material from poly(copper phthalocyanine) (Poly-CuPc) and multi-walled carbon nanotubes (MWCNTs). The optical behaviour of the hybrid material was red-shifted (longer wavelengths), with improved absorption intensity & increased charge transfer between Poly-CuPc moieties and CNT walls in the UV/vis spectrum. With numerous conductive channels for charge carriers, CNTs play a significant role in improving the electrical conductivity of the hybrid material. Further, Atomic Force Microscopy (AFM) studies not only showed that the excess of interfacial contact between Poly-CuPc and CNTs was evident, but also surface roughness and complexity increased due to CNT integration over the Poly-CuPc layer. Thus, it favours the idea that the inclusion of CNTs has considerably altered the surface morphology of Poly-CuPc. The photoelectronic properties of the hybrid material on Si/SiO2 substrate were studied, wherein it was observed that much higher photocurrent was obtained as compared to dark current under illumination of light over uncoated Poly-CuPc. We applied an electric potential ranging from −5 V to +5 V to the sample under different experimental conditions to investigate the influence of voltage on both photoelectrical and insulating responses. A 120 W yellow lamp (intensity of ≈ 38.2 Wm^{-2}; radiation wavelength of ≈ 580 nm). The light was directed onto a small (6 cm^2) rectangular sample area. Five repetitions were performed to ensure the precision of the results. The Experiment was performed during winter at 25 °C and 30% humidity. Dark and light currents of (2.50×10^{-6}, 1.33×10^{-6}) and (5.60×10^{-6}, 6.04×10^{-6}) amperes for poly-CuPc as well as for Poly-CuPc/MWCNT were characterized in this work. In addition, the data indicated a solid response when 10% MWCNT was added to the sample. More importantly, CNTs dramatically increased the DC conductivity, providing effective charge-transport pathways and improving electrical performance.

How to cite this article
Abduljawad .J, Banimuslem .H. Multi Walled Carbon Nanotubes Incorporated Poly-Copper Phthalocyanine as Nano Composite Thin Films Deposited on Silicon-Silicon Dioxide Substrate for Photocurrent Efficiency. J Nanostruct, 2026; 16(3):4234-4248. DOI: 10.22052/JNS.2026.03.104

* *Corresponding Author Email:*
benin.kadhim561@student.uobabylon.edu.iq

This work is licensed under the Creative Commons Attribution 4.0 International License.
To view a copy of this license, visit http://creativecommons.org/licenses/by/4.0/.

INTRODUCTION

The rapid development of nanotechnology has not kept pace with demand, and a growing range of substances with mechanical, optical, or electrical characteristics has become essential to meet these demands. Among the wide variety of hybrid materials, these new technologies are emerging from the interaction of two or more efficient components [1, 2]. Furthermore, research concerning the interaction of carbon nanotubes with conjugated polymeric molecules – mainly metal phthalocyanine (MPc) began attracting more interest in the last few decades as a new topic of fundamental research with potential applications from sensing to photovoltaic ones [3].

Taking advantage of the excellent electrical, thermal, and mechanical properties of Carbon nanotubes, as well as the characteristics of optoelectronics of MPc, is an ideal route to fabricate composite materials that can greatly enhance relative responses compared with pristine carbon nanotubes CNTs. Phthalocyanines (Pcs) and their metallo-derivatives (MPc) generally represent a class of materials with pronounced potential for the fabrication of several nonlinear optical devices due to their optical limiter behavior, fast response time, peculiar electronic absorption features, and an extremely delocalized π-π electron skeleton [5]. Another advantage of MPCs is that they can be processed into thin films and, once again, deposited by various techniques, including spin-coating, drop-casting, thermal evaporation, and Langmuir-Blodgett deposition. Substituted-MPc has also been used as an active membrane in surface plasmon resonance (SPR) and total internal reflection ellipsometry (TIRE) sensors [6].

MPcs are π-electron-conjugated macrocyclic compounds with excellent potential for applications in chemical and biosensors, liquid crystals, field-effect transistors, electrochromic devices, and memory applications. Device performance is influenced by the structure of MPcs, which affects their attributes (such as specific surface area, electron-transfer characteristics, and thermal stability) [7]. The strongest advantages of MPcs over their organic analogs are: (i) A tunable structure, having a great flexibility in introducing different substituents to the periphery of rims well as in coordinating nearly every metallic element in the middle of macrocycle; (ii) An exceptional thermal and chemical stability if compared with most molecular materials; (iii) The possibility to make a large variety of thin films by distinct deposition methods [8]. lthough MPc-based devices have been studied for a long time, some specific limitations still need to be overcome including (1) improving the reproducibility of organic thin film devices due to poor control on the crystallite orientation of polycrystalline MPc film, (2) enhancing selectivity and sensitivity of MPc thin films sensors, (3) providing more homogenous films in manufacturing semiconductor films without pin-holes that can lead to short circuit problems, and (4) increasing charge carrier mobility in organic thin film diode or transistors which is strongly determined by various factors such as type, orientation and structure of MPcs together with its film thickness and nature of interface between organic film diamagnetic electrodes [9,10].

CNTs exhibiting a high aspect ratio are π-conjugated nanomaterials, in contrast. This class of carbon materials exhibits numerous advantageous mechanical, thermal, and electrical properties; therefore, this carbon structure is an excellent candidate for various applications, such as a reinforcing filler in polymers, a component of heat-management equipment, and a substrate material for nanoelectronic devices [11,12]. CNTs are known to be highly sensitive to their surrounding chemical environment. The wide applications of CNTs can be attributed to their superior electrical properties, small size, extremely high surface-to-volume ratio, and strong adsorption capacity [13,14].

However, the low solubility and dispersibility of CNTs in common solvents have limited their use as active layers via easy methods such as spin coating. Acid treatment and other modification methods, such as mixing with organic dyes, can also be used to address shortcomings in poorly dispersed CNTs. Another drawback is that CNTs are optically passive and very difficult to use as an active layer in photocurrent, photovoltaic, and optical detection methods, as well as in any application that requires light absorption [3]. In addition, the surface modification of CNTs through hybridization with MPcs can improve their photocurrent and photovoltaic performance due to π-π stacking interactions between CNTs and MPcs, which are more effective than either of the individual species or MPcs [2,17,18].

This study focuses on the fabrication of Poly-

CC BY

CuPc/MWCNT hybrid thin films deposited on silicon/silicon dioxide to investigate photocurrent performance and to perform complementary characterizations, including optical absorption and morphology.

MATERIALS AND METHODS

The synthesis of the hybrid materials for this study, poly(copper phthalocyanine) and multi-walled carbon nanotubes (MWCNTs), is further described below. Before the clean-up process substrate required elimination of pollutants or impurities the first step, was performed by cleaning the substrate with distilled water followed by clean up with laboratory ethanol. Then, 10 mg of poly(copper phthalocyanine) was weighed and dissolved in dimethyl sulfoxide (DMSO) (400 mL). Club member Cynthia Fischer used copper phthalocyanine and the solvent in a 5/4 (solvent to poly) ratio, and after agitating at RT for 30 minutes, found that the poly (copper phthalocyanine) was completely dissolved. Weighing 9 mg of poly(copper phthalocyanine) and diluting it in 300 millilitres of DMSO, the hybrid sample was spun until completely dissolved. Then, 1mg of MWCNTs was resuspended in 100ml of DMSO and shaken for 30 minutes to ensure homogeneous distribution. Dropwise addition of a suspension of MWCNTs to a poly(copper phthalocyanine) solution yields hybrid materials containing 10 weight percent MWCNTs. To ensure uniform dispersion of poly(copper phthalocyanine) and MWCNTs, the hybrid samples were sonicated for 30 min after preparation.

Next, the samples were subjected to 15 minutes of liquid grinding in a mechanical grinder to achieve homogeneity and surface functionalization of MWCNTs and poly(copper phthalocyanine). The hybrid material was drop-cast onto ITO glass for IV measurements and onto a Si/SiO2 substrate for photocurrent measurements. The drop-dry-drop method was applied during drop casting to ensure complete substrate coverage. The top electrode was made using a silver paste, allowing current to be efficiently transmitted between electrodes and ensuring good electrical contact with the active layer (Fig. 1).

These conditions were repeated 4 times to assess reproducibility, and they were highly reproducible. The measurements are repeated 5 times for each sample, and it is quite obvious that the devices are highly reversible.

The optical properties of the samples were studied by analyzing their absorption spectra in the UV and visible wavelength ranges using UV-Visible absorption spectroscopy. The IV measurement and photocurrent of the samples were carried out using Kiethley 2400 source meter. The light used in this work was a 120-watt halogen. The photocurrent experiment was performed using a time-dependent program interfaced with the source meter. The thickness of all thin films prepared was measured using an optical refractometer.

RESULTS AND DISCUSSION

UV-Visible Spectra

Of the numerous metallophthalocyanine derivatives, poly-copper phthalocyanine (Poly-CuPc) has proven to be one of the most stable and optically active. This compound belongs to a class of planar aromatic macrocycles with a central Poly-CuPc/CNT. These macrocycles are characterized by their intense π→π* electronic transitions within the conjugated frame and outstanding thermal stability[19,20]. At the interface of the Poly-CuPc component and nanoparticles, the charge delocalization across conjugated rings becomes increased with enhanced interfacial π–π stacking interactions between graphitic walls of CNTs embedded with Poly-CuPc. Due to these interactions, the Optical absorption intensity and electrical conductivity are extremely high, making the Poly-CuPc/CNT solution suitable for advanced

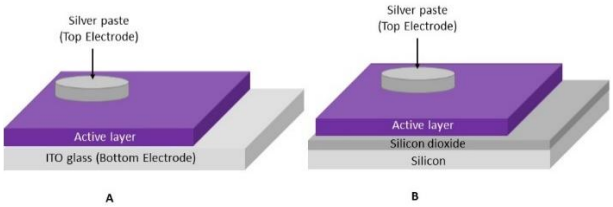


Fig. 1. The devices prepared in this work.

CC BY

optoelectronic devices [21,22].

The section below compares the UV-Vis absorption spectra of pure Poly-CuPc and pure CNT-deposited samples to better understand the optical evolution imparted by nanotube incorporation [23].

Fig. 2. The spectra reveal the signature B-band in the near-UV (≈330–380 nm) and Q-band in the visible region (≈600–700 nm) owing to π→π* transitions within the conjugated phthalocyanine macrocycle. With the incorporation of carbon nanotubes (CNTs) into pure Poly-CuPc solution, the characteristic Q-band ($\Delta\lambda > 0$) is significantly redshifted, and the absorption strength is proportionally heightened while maintaining a slight widening. Collectively, these signals facilitate electronic delocalization through their compatibility with π–π stacking at the interface and charge-transfer coupling between the Poly-CuPc chromophores and the graphitic CNT walls. J-type excitonic coupling, or the generation of charge-transfer states, is typically inferred from a red-shifted, slightly broadened Q-band, while an increase in the B-to-Q intensity ratio indicates an overall rise in the composite's oscillator strength. Additionally, any low-energy tailing (if present)

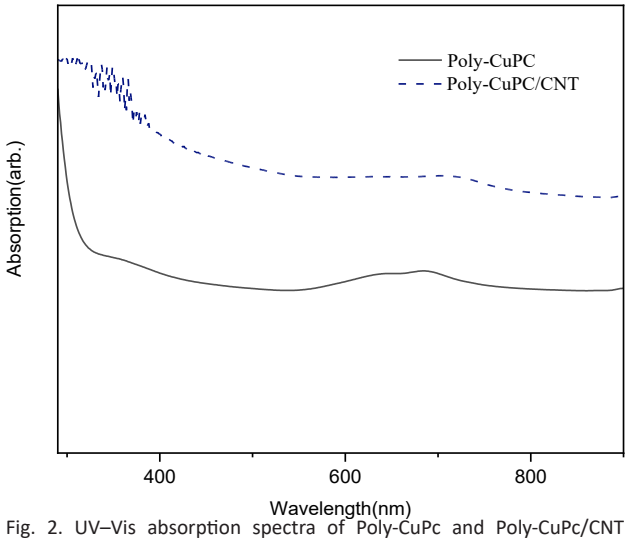


Fig. 2. UV–Vis absorption spectra of Poly-CuPc and Poly-CuPc/CNT solutions in DMSO.

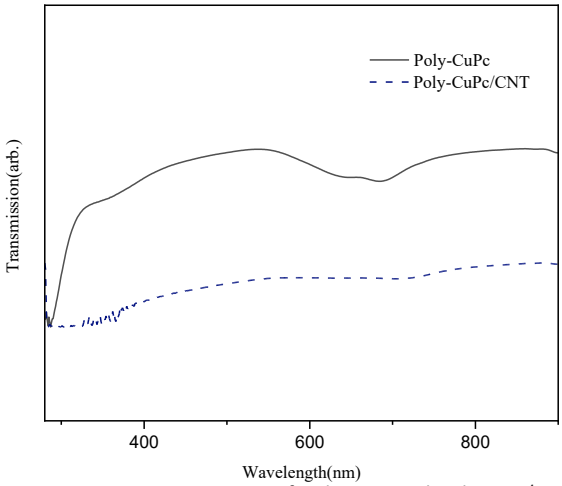


Fig. 3. Transmittance spectra of Poly-CuPc and Poly-CuPc/CNT solutions in DMSO.

CC BY

toward longer wavelengths may indicate donor-acceptor interactions occurring between the CuPc macrocycles (donor) and the CNTs (acceptor) in order to have a fair comparison both spectra have been treated according to the same baseline correction and normalization procedures, ensuring that spectral evolution observed is solely as a result of CNT corporation and not due to concentration or path-length distortions.

To evaluate the effect of carbon nanotube incorporation on the transparency of the obtained phthalocyanine samples, the room-temperature optical transmittance behavior was studied over the 300–900 nm spectral range. The acquired spectra reveal two distinct zones of transmission associated with the Q-band in the visible (~620–690 nm) and B-band in the near-UV region (~330–380 nm). These results confirm the intrinsic molecular characteristics of the phthalocyanine macrocycle by directly correlating with the π→π* electronic transitions previously detected in absorption spectra [24].

Fig. 3. The transmittance of Poly-CuPc and its CNT-doped counterpart clearly shows that there is a significant difference in optical transparency upon the integration of nanotubes. The black solid line, corresponding to the pristine Poly-CuPc, indicates a homogeneous dispersion of the polymeric phthalocyanine species in solution. It shows shallow peaks and troughs in light transmission across the visible spectrum. In contrast, the transmittance intensity of Poly-CuPc/CNT composite (purple dashed line) suffers a rather broad decrease across the whole spectrum.

The optical reflectance of phthalocyanine-based polymers provides much information about their electronic structure and the interaction of surfaces with incident light. Because of the strong absorption in their π--π* transition bands, metallophthalocyanines (MPcs) generally have relatively low reflectance in the visible region[20,25]. This feature arises from the significant conjugation of delocalized π-electrons across planar macrocyclic frameworks, enabling efficient light absorption rather than reflection. The optical response of these semiconducting macrocycles is dominated by basic molecular excitations, embodied in the characteristic Q- and B-bands commonly observed at 600–700 nm and 330–380 nm, respectively[26].

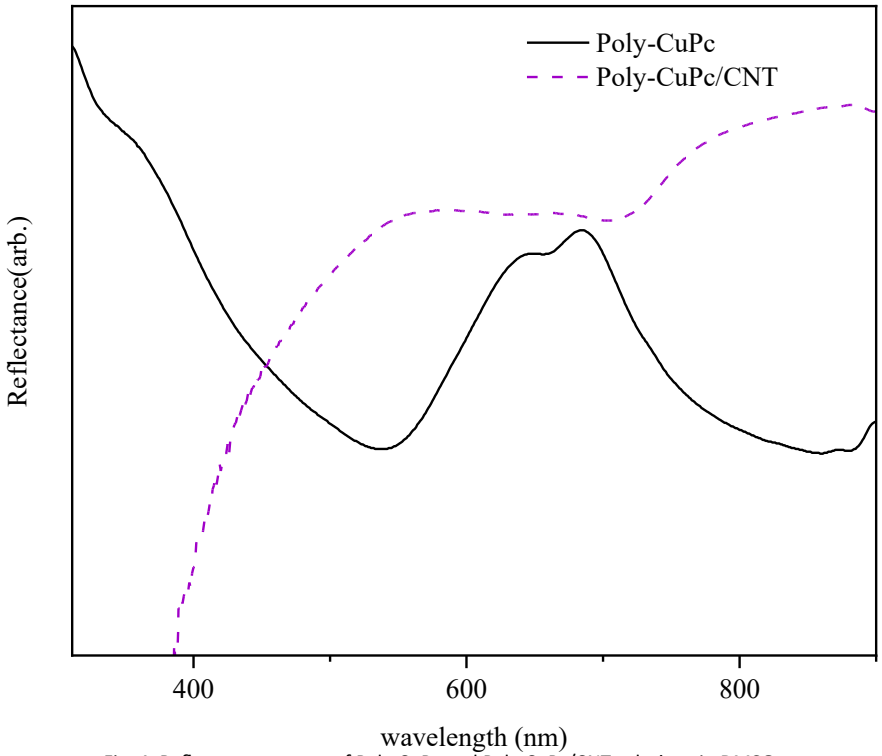


Fig. 4. Reflectance spectra of Poly-CuPc and Poly-CuPc/CNT solutions in DMSO.

Fig. 4 In the reflectance spectra of Poly-CuPc and its CNT-modified composite, we can see optical effects related to the added carbon nanotubes. This also confirms the large absorption capacity of phthalocyanine molecules, as evidenced by low reflectance in the visible spectrum for pure Poly-CuPc, shown by the black solid curve. It can also be seen in the 2 faint reflection peaks adjacent to B and Q, respectively, revealing molecular excitations that form the conjugated macrocyclic scaffold. The purple dashed curve shows an overall increase in reflectance intensity after loading carbon nanotubes, particularly in the 500-800 nm range. This modification indicates that the CNTs alter the geometric and optical path of the material, thus causing greater photonic diffuse reflection at regions configured by the polymeric phthalocyanine chains and nanotubes.

For semiconducting materials, the optical energy gap (Eg) is a crucial factor in determining their electrical properties. The band gap of metallophthalocyanines (MPcs) is primarily governed by the delocalized π–π* electronic transitions of their conjugated macrocyclic motif. Its magnitude determines the onset of optical absorption and the suitability for optoelectronic and photovoltaic applications [27]. This notable adjustment in the energy gap occurs due to interactions with the π-electron systems of both components when carbon nanotubes (CNTs) are introduced into the phthalocyanine matrix [28]. The extended conjugation and strong electrical conductivity of CNTs allow charge transfer and an overlap between orbitals with the neighboring phthalocyanine molecules, which generally leads to a slightly diminished optical band gap[29]. This

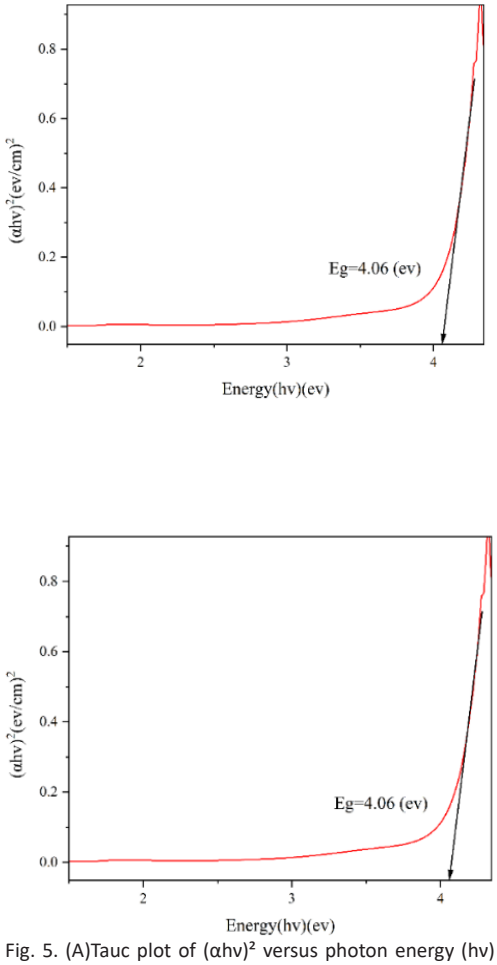


Fig. 5. (A)Tauc plot of $(\alpha hv)^2$ versus photon energy (hv) for pure poly-CuPc sample. (B) Tauc plot of $(\alpha hv)^2$ versus photon energy (hv) for poly-CuPc/CNT hybrid sample.

CC BY

means that more states are available for electron delocalization across the hybrid interface, as CNTs introduce new electronic states near the Fermi level [30]. The Tauc equation, which explains the connection between the absorption coefficient and the photon energy, was utilised to determine the optical band gap [34]:

$$\alpha = A(hv - Eg)^{1/2}/hv \quad (1)$$

Where α, E_g, and A stand for the absorption coefficient, band gap, and constant, respectively. The samples were liquid, and the cuvette thickness was 1 cm. The absorption coefficient was calculated according to the Eq. 2 [34]:

$$\alpha = \frac{2.303\ A}{t} \quad (2)$$

Where A is the absorption and t is the thickness.

Phthalocyanine typically has two absorption regions: one in the visible and the other in the near-UV. Fig. 5 shows the energy gap calculated from the higher-absorption region near the UV.

As per the result depicted in Fig. 5(A), the optical bandgap of poly-CuPc exhibits a sharp linear part corresponding to a direct allowed transition. From this part, the optical energy gap (Eg) was calculated to be 4.10 eV. This relatively large band gap suggests the insulating characteristics of the poly- CuPc structure and limited molecular orbital overlap in the π-conjugated system. Fig. 5(B) also reveals that the energy band gap was considerably lower, at 3.18 eV, after the incorporation of CNTs into the poly-CuPc matrix [35].

IV measurements

Fig. 6 represents the I-V characteristics of Poly-CuPc and Poly CuPc/CNT thin films deposited on ITO glass as the bottom electrode, and the top electrode was silver, as represented in Fig. 1(A). The conductivity was calculated from the fitting information in Fig. 6 through the following equation:

$$\sigma = \frac{d}{RA} \quad (3)$$

Where σ is the conductivity measured in $\Omega^{-1}m^{-1}$, d is the film thickness, A is the cross-sectional area of the top electrode (3.01×10^{-9} m^2), and R is the resistance, which equals $slope^{-1}$. These curves are quite useful because they indicate a material's behavior at different voltages by representing the

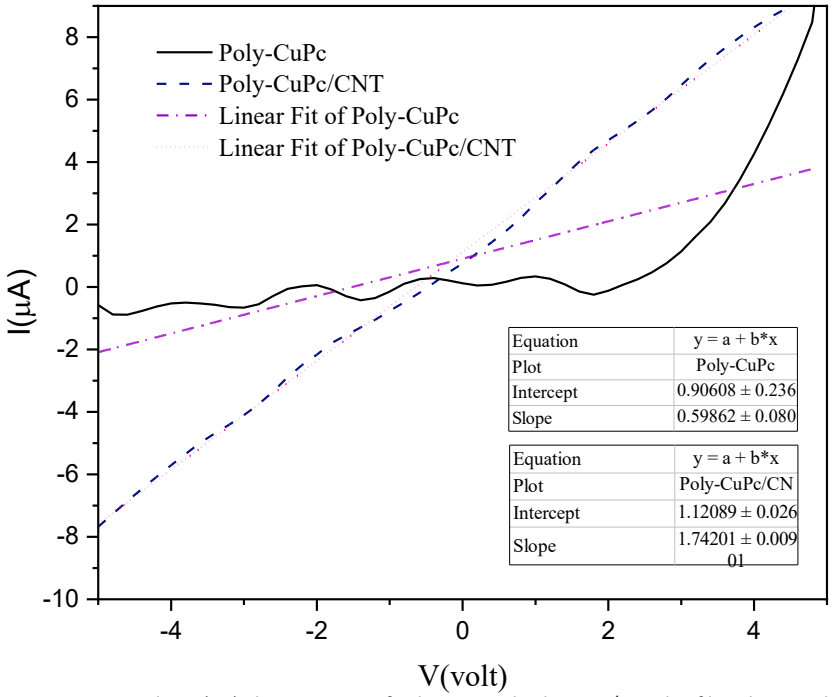


Fig. 6. Current-Voltage (I-V) Characteristics of Poly-CuPc and Poly- CuPc/CNT thin films deposited on ITO glass.

CC BY

relationship between current and applied voltage. See the Fig. 6.

The conductivity values are represented in Table 1. The conductivity of Poly-CuPc/CNT is clearly higher than the conductivity of Poly-CuPc. The doping of organics with CNTs has been extensively studied due to the superior electrical and optical properties of CNTs. Specifically, Poly-CuPc is a viable option as a typical organic semiconductor for optoelectronic devices, such as photodetectors [36,37]. The addition of CNTs, which have superior electrical conductivity and mechanical properties, could enhance the electrical behavior of organic materials for optoelectronics. When CNTs are mixed with Poly-CuPc, the combined product is known to exhibit higher electrical conductivity than pure Poly-CuPc [38]. This improvement is attributed to the conductive CNTs, which facilitate

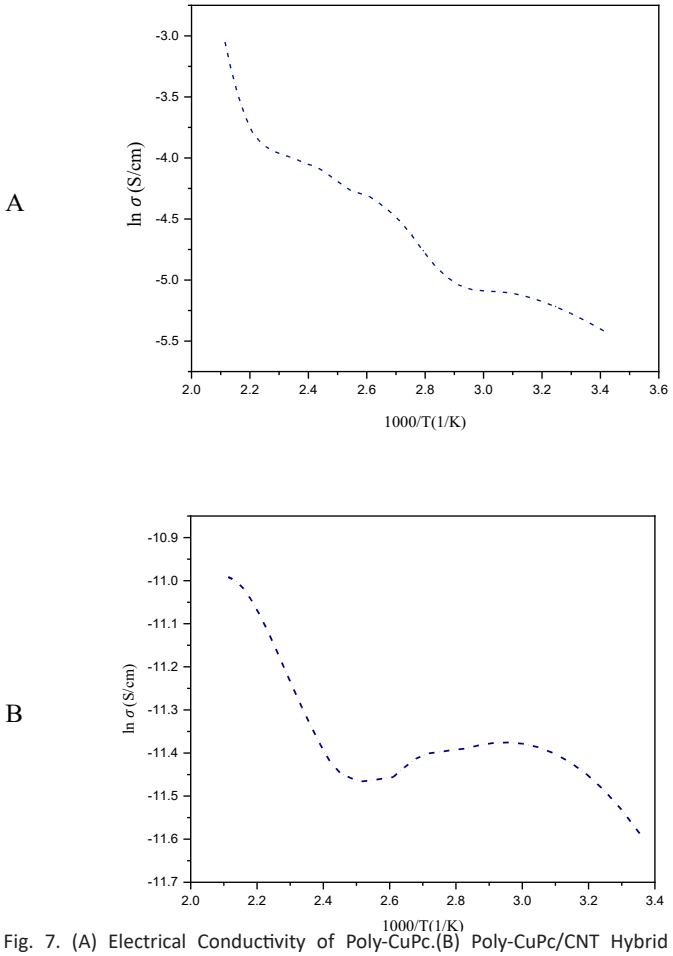


Fig. 7. (A) Electrical Conductivity of Poly-CuPc.(B) Poly-CuPc/CNT Hybrid Materials.

Table 1. Conductivities of Poly-CuPc and Poly-CuPc/CNT thin films.

Sample	Slope (fig.6)	R (Ω)	Film thickness	Conductivity ($\Omega^{-1}m^{-1}$)
Poly-CuPc	0.59×10^{-6}	5.4×10^{5}	200 nm	3.9×10^{-5}
Poly-CuPc/CNT	1.74×10^{-6}	2.6×10^{5}	250 nm	1.4×10^{-4}

CC BY

charge percolation through the hybrid material, thereby yielding a stronger linear response in its I-V characteristics. The addition of CNTs forms a conductive network that facilitates more efficient electron transfer, thereby increasing current density at the same voltage. This is consistent with reports in the literature, which show that adding CNTs to organic semiconductors can significantly increase electrical conductivity. See the Table 1.

DC Conductivity

Phthalocyanines, a class of macrocyclic organic compounds characterized by extensive π-conjugation and outstanding chemical stability, exhibit excellent electronic and optoelectronic properties [31]. These characteristics make phthalocyanines possible candidates for use in organic electronics, photovoltaic cells, and sensing devices—all of which rely on charge transfer or electrical conductivity. Poly Copper phthalocyanine (Poly-CuPc) and its derivatives are by far the most studied class of phthalocyanines, especially due to their reproducible thin-film formation, stability, and potential electron donors in organic electronic devices. As promising as phthalocyanine films are, their electrical conductivity can be too low to give high performance [32]. In this regard, combining phthalocyanines with highly conductive nanostructures, such as carbon nanotubes (CNTs), to prepare hybrid composites has attracted increasing attention from researchers. Due to their strong π-electron interactions, large aspect ratio, and extraordinary electrical conductivity, carbon nanotubes are an ideal charge-transport medium in hybrid-design polymers.The conductivity was calculated using the Eq. 4:

$$\sigma = \frac{L}{RHWN} \tag{4}$$

Where (*H*) is the film thickness, (*L*) is the gap between fingers, (*W*) is the overlap distance between the electrodes, (*Nr*) is the number of fingers of interdigitated electrodes, and (R) is the film's resistance. The temperature dependence of the electrical conductivity of the materials can be analyzed by the Arrhenius equation [32]:

$$\sigma = \sigma_o \exp\left[\frac{E_a}{K_B T}\right] \tag{5}$$

Where (σ_o) is constant, (E_a) is the activation energy, (K_B) is the Boltzmann constant equal to (1.38 ×) J/K, and T is the temperature in Kelvin. From the above equation, we can write the activation energy equation as:

$$Ea = \frac{T \times Ln\sigma}{1000} \times K_B \times 1000 \left(\frac{J}{K}\right) \tag{6}$$

Fig. 7A shows the electrical conductivity of poly-copper phthalocyanine (Poly-CuPc) as a function of temperature, indicating the semiconducting properties of the material. Conductivity of the hybrid material after adding Poly-CuPc incorporated with carbon nanotubes (CNTs) is shown in Fig. 7B. Addition of CNTs, which inherently have very high conductivity and provide more channels for charge transfer, will increase conductivity significantly. This leads to high electron mobility and low conduction-path barriers, which benefit the electrical performance of a hybrid system. These findings demonstrate that adding nanoparticles enables organic materials to achieve improved electrical properties suitable for next-generation electronic devices.

Scanning Electron Microscope (SEM)

Fig. 8 represents the SEM images of poly copper phthalocyanine (a) and its hybrid with carbon nanotubes (b). Phthalocyanine and their derevitives always tend to form featureless morphology films as appears in scanning electron microscopy images. However, after adding carbon nanotubes there was an obvious interaction between two materials as image (b) shows. Mixing phthalocyanine with carbon nanotubes not only modify phthalocyanine but also shortening the

Table 2. Activation energy (eV) of Poly-CuPc and Poly-CuPc/CNT Hybrid Materials.

Sample	Activation energy (eV)	
	E_{a1}	E_{a2}
Poly-CuPc	0.2107	0.0636
Poly-CuPc/CNT	0.1174	0.0403

CC BY

tubes and makes the hybrid more convenient for easy processing applications [39].

Atomic Force Microscopy

Fig. 9 represents the Atomic force microscopy images of 9(A) Poly-CuPc thin film and 9(B) Poly-CuPc/CNT film. This method enables high-resolution analysis of surface morphology (RMS roughness, growth orientation, and layer uniformity) for the structural characterization of films, as AFM provides three-dimensional (3D) surface topography at high spatial resolution without requiring complex sample preparation [40]. From the images, the surface morphology of phthalocyanine appears homogeneous and particle-like, with a surface roughness of

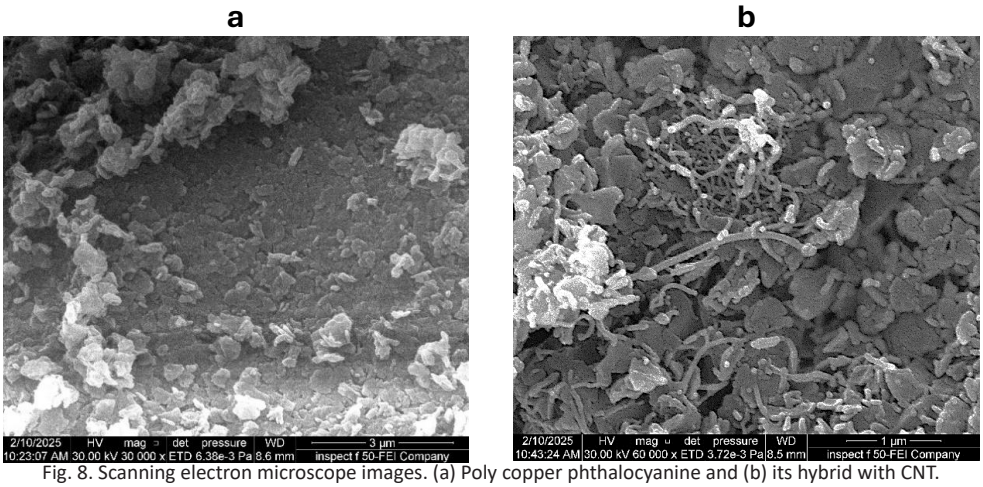


Fig. 8. Scanning electron microscope images. (a) Poly copper phthalocyanine and (b) its hybrid with CNT.

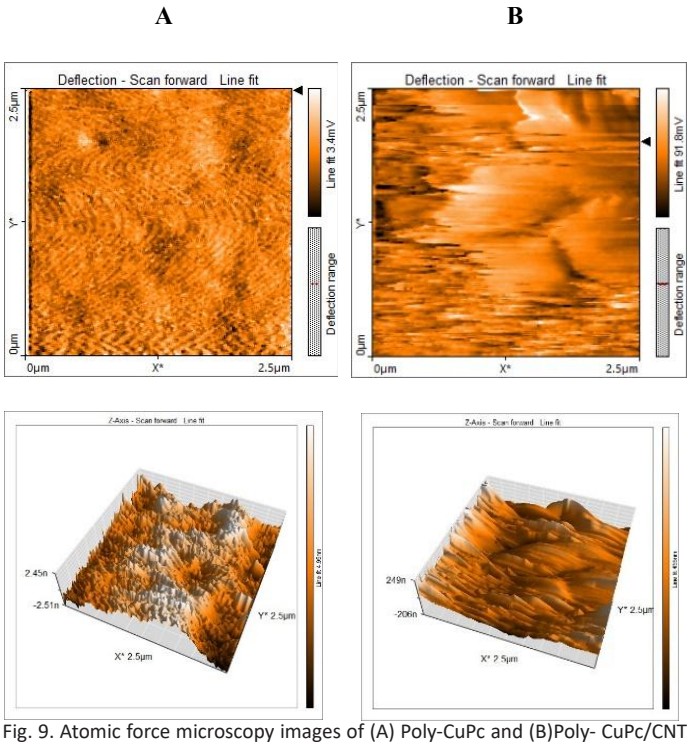


Fig. 9. Atomic force microscopy images of (A) Poly-CuPc and (B)Poly- CuPc/CNT thin films.

CC BY

approximately 15.35 nm. Phthalocyanines and their metallo-derevatives tend to form homogeneous thin films on substrates in any processing method [16]. Figure 9 (B) represents the image of carbon nanotubes. CNTs typically increase film roughness because they are one-dimensional materials [18]. The roughness of the Poly-CuPc/CNT samples is measured at 89.02 nm. This increase in roughness has contributed to a larger surface area and a higher photocurrent response. See the Fig. 9. The RMS values were 22.5 nm and 106 nm for the Poly-CuPc and Poly-CuPc/CNT samples, respectively. The grain size was in the range of 280-380 nm.

Photocurrent (Photoconductivity)

The photoresistive properties of the Poly-CuPc/CNT hybrid were studied to determine its light responsivity. The change in photoresistance was used to assess the impact of light on the material's electrical conduction behaviour. The observation of an apparent photoresponse to light irradiation renders the material interesting for optical sensing [41]. Fig. 10 represents the time dependence of the current response due to light radiation. From this figure, it is clear that the response is large in both samples, with and without carbon nanotubes. However, the Poly-CuPc sample was irreversible,

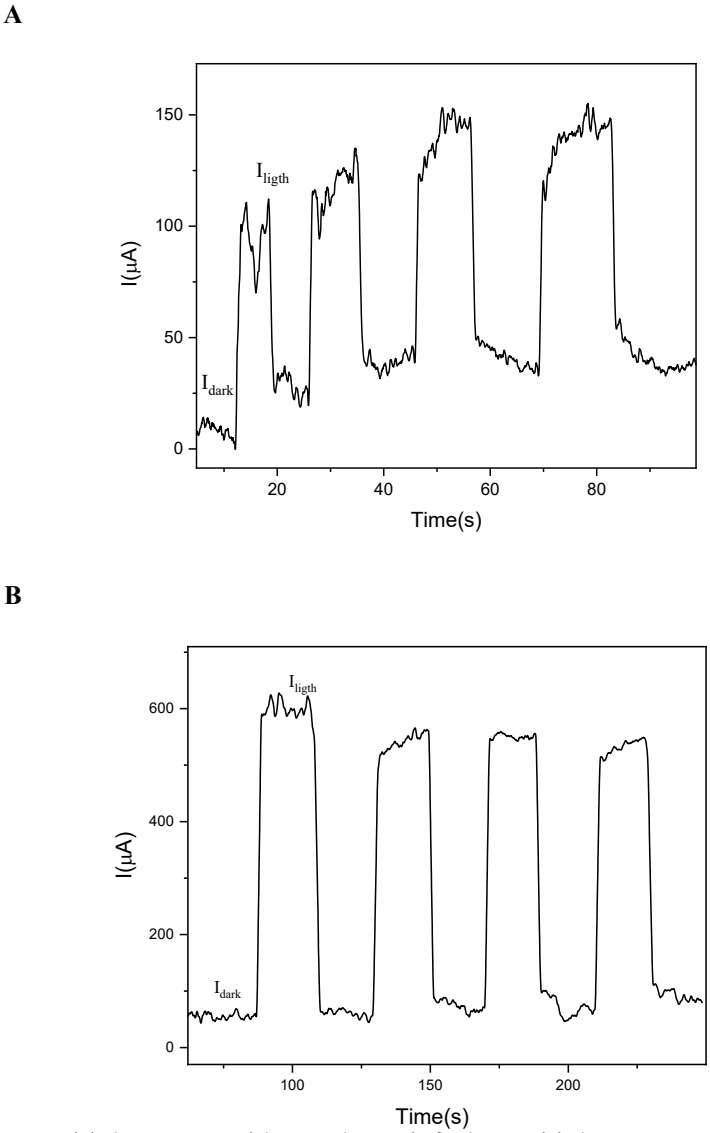


Fig. 10. (A) Photoresistance (Photoconductivity) of Poly-cuPc, (B) Photoresistance (Photoconductivity) of Poly-cuPc/CNT Hybrid.

CC BY

whereas the Poly-CuPc/CNT sample was reversible and stable over time. This observation is attributed to the electron channel formed in the composite upon interaction between the phthalocyanine and the carbon nanotube channel, which prevents electron penetration into the materials, leading to saturation and irreversibility in the Poly-CuPc sample. See the Fig. 10.

The photoresistivity and current response to light were calculated from the matching information included in Fig. 9 using the following equations [42]:

$$I_{photo} = I_{light} - I_{dark} \quad (7)$$

Where I_{photo} is the photocurrent, I_{light} is the current measured under illumination, and I_{dark} is the dark current. This relationship immediately corresponds to the number of created carriers by absorption of a photon. The relative increase in the current due to illumination can be expressed in terms of the sensitivity of the material towards

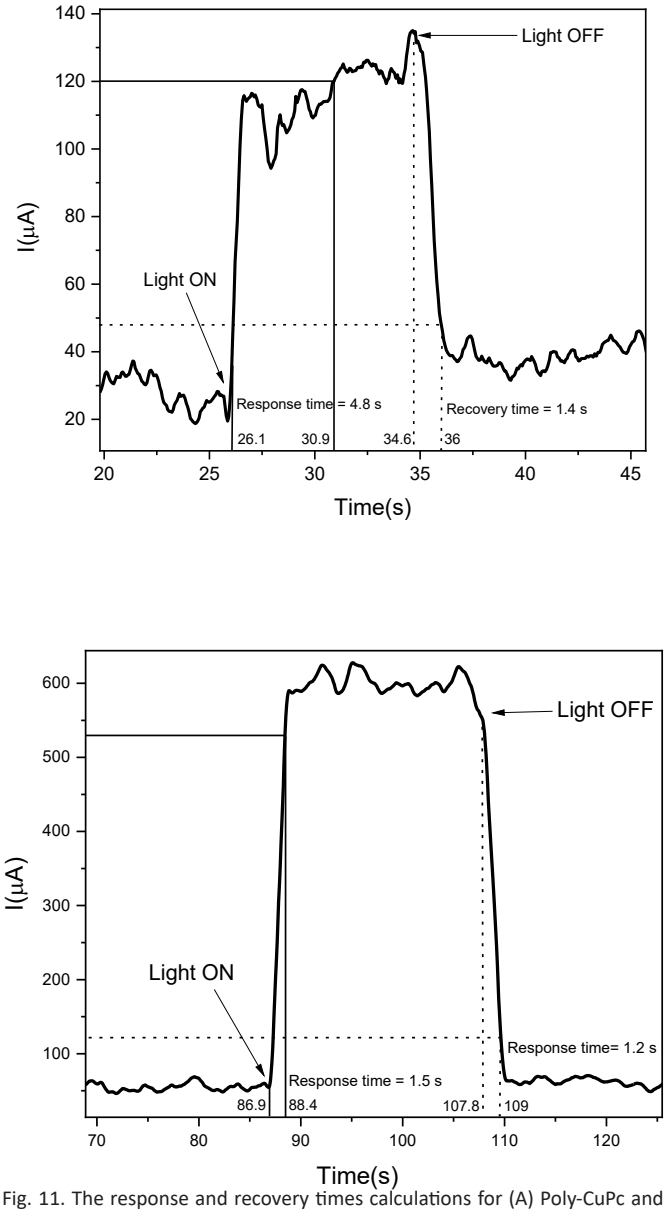


Fig. 11. The response and recovery times calculations for (A) Poly-CuPc and (B) Poly-CuPc/CNT.

CC BY

Table 3. Photoconductive and photoresponse parameters of Poly-CuPc and Poly-CuPc–CNT photodetectors.

Parameters	Poly-CuPc	Poly-CuPc-CNT
I_{dark}(μA)	2.50	5.60
I_{light}(μA)	1.33	6.04
I_{photo}(μA)	1.08	5.48
Response %	432%	979%
Responsivity(A/W)	9.00	4.57
External quantum efficiency(EQE)	1.29	9.79
Response time (s)	4.8	1.5
Recovery time (s)	1.4	1.2

optical excitation, either photoresponse or sensitivity PS (%):

$$PS(\%) = \frac{I_{light} - I_{dark}}{I_{dark}} \times 100\% \quad (8)$$

This parameter provides a normalized measure of the material's response to incident radiation.

Another important parameter for characterizing photodetector performance is responsivity (R_λ) [42]

$$R_\lambda = \frac{I_{photo}}{P_{opt}} \quad (9)$$

Where P_{opt} is the incident optical power, a larger responsivity implies a better photon-to-current conversion.

The EQE (external quantum efficiency) characterizes how well incident photons are converted to charge carriers and is connected to responsivity by:

$$EQE = \frac{hc}{q\lambda} R_\lambda \quad (10)$$

Where h is the Planck constant, c is the speed of light, q is the elementary charge in coulombs, and λ is the wavelength of input light [43].

A photogenerated current arises from photon absorption and subsequent electronic transitions—quantum phenomena. When photons strike the material, electrons absorb discrete energy quanta and move from lower to higher energy levels. This excitation generates free carriers, thereby altering electrical conductivity. The effectiveness of this process is influenced by photon energy, material morphology, and charge transport [44]. The response time and recovery time describe the dynamic properties of the photodetector. The response time is the time required to reach a specified fraction (usually 90%) of its steady-state value after illumination, and the recovery time is the time required to decay once the light source has been removed. These parameters quantify the rates of carrier generation and recombination [45,46]. Fig. 11 clarifies the calculations of response and recovery times. All the calculations discussed are presented in Table 3. See the Fig. 11.

CONCLUSION

The optical and electrical properties of the composite differ because it is a combination of carbon nanotubes (CNTs) and poly(copper phthalocyanine) (Poly-CuPc). This is due to the electronic interactions between Poly(copper phthalocyanine) (Poly-CuPc) and the nanotube walls, which are responsible for the red-shifted absorption edge and increased composite extinction coefficient. This enhances its potential for photonic materials, sensing applications, and light absorption in the visible-UV range. Moreover, the photoresistive characterizations show that upon red-light stimulation, the responsiveness of the Poly-CuPc/CNT composite is considerably higher than that of pure Poly-CuPc. This indicates that the electrical conductivity and photoresponse of DMSO-silica composites are enhanced, which

CC BY

is favorable for solar cell devices and ultra-high-sensitivity photodetectors. The CNTs significantly improved the DC conductivity of the Poly-CuPc composite. Importantly, the additional conductive channels through which CNTs operate can all smooth electron flow, increasing the overall DC conductivity of the hybrid material. We attribute these gains in conductivity to the Poly-CuPc/CNT hybrid being more advantageous for high-performance electronics (e.g., energy harvesting, photodetection). The significantly higher photoresponse is attributed to additional charge-transfer channels induced by the increased number of CNTs. Such channels can provide effective electron-hole separation under light irradiation, enabling fast response times and higher sensitivity in photonic sensing applications. In addition, these results are consistent with AFM measurements indicating a significant change in the surface morphology of Poly-CuPc thin films upon CNT doping, which favors charge transfer and interfacial contact [14]. These morphological changes validate the beneficial role of Poly-CuPc/CNT composites on optical absorption, electrical conductivity, and photoresponse.

CONFLICT OF INTEREST

The authors declare that there is no conflict of interests regarding the publication of this manuscript.

REFERENCES

1. Karnwal A, Kumar Sachan RS, Devgon I, Devgon J, Pant G, Panchpuri M, et al. Gold Nanoparticles in Nanobiotechnology: From Synthesis to Biosensing Applications. ACS Omega. 2024;9(28):29966-29982.
2. Ramachandran T, Ali A, Butt H, Zheng L, Deader FA, Rezeq Md. Gold on the horizon: unveiling the chemistry, applications and future prospects of 2D monolayers of gold nanoparticles (Au-NPs). Nanoscale Advances. 2024;6(22):5478-5510.
3. Mohammed MS, Al-Rubae'i SHN, Rheima AM, Al-Kazazz FF. A novel sandwich ELISA method for quantifying CHI3L1 in blood serum and cerebrospinal fluid multiple sclerosis patients using sustainable photo-irradiated zero-valence gold nanoparticles. Results in Chemistry. 2024;11:101856.
4. Gu X, Xu Z, Gu L, Xu H, Han F, Chen B, et al. Preparation and antibacterial properties of gold nanoparticles: a review. Environ Chem Lett. 2020;19(1):167-187.
5. Hammami I, Alabdallah NM, jomaa AA, kamoun M. Gold nanoparticles: Synthesis properties and applications. Journal of King Saud University - Science. 2021;33(7):101560.
6. Canning AJ, Li JQ, Atta S, Wang H-N, Vo-Dinh T. Nanoplasmonics biosensors: At the frontiers of biomedical diagnostics. TrAC, Trends Anal Chem. 2024;180:117973.
7. Khelifa L, Hu Y, Jiang N, Yetisen AK. Lateral flow assays for hormone detection. Lab on a Chip. 2022;22(13):2451-2475.
8. Guliy OI, Dykman LA. Gold nanoparticle–based lateral-flow immunochromatographic biosensing assays for the diagnosis of infections. Biosensors and Bioelectronics: X. 2024;17:100457.
9. Soh JH, Chan H-M, Ying JY. Strategies for developing sensitive and specific nanoparticle-based lateral flow assays as point-of-care diagnostic device. Nano Today. 2020;30:100831.
10. Farka Z, Brandmeier JC, Mickert MJ, Pastucha M, Lacina K, Skládal P, et al. Nanoparticle-Based Bioaffinity Assays: From the Research Laboratory to the Market. Adv Mater. 2023;36(3).
11. Jin Z, Yim W, Retout M, Housel E, Zhong W, Zhou J, et al. Colorimetric sensing for translational applications: from colorants to mechanisms. Chem Soc Rev. 2024;53(15):7681-7741.
12. Butt A, Bach H. Nanomedicine and clinical diagnostics part I: applications in conventional imaging (MRI, X-ray/CT, and ultrasound). Nanomedicine. 2024;20(2):167-182.
13. Aslan N, Ceylan B, Koç MM, Findik F. Metallic nanoparticles as X-Ray computed tomography (CT) contrast agents: A review. J Mol Struct. 2020;1219:128599.
14. Mutreja I, Maalej N, Kaushik A, Kumar D, Raja A. High atomic number nanoparticles to enhance spectral CT imaging aspects. Materials Advances. 2023;4(18):3967-3988.
15. La Riviere P. Accurate analytic reconstruction in X-ray fluorescence computed tomography. Proceedings IEEE International Symposium on Biomedical Imaging: IEEE. p. 637-640.
16. Díaz-Galindo CA, Garnica-Garza HM. Gold nanoparticle-enhanced radiotherapy: Dependence of the macroscopic dose enhancement on the microscopic localization of the nanoparticles within the tumor vasculature. PLoS One. 2024;19(7):e0304670.
17. Mitchell MJ, Billingsley MM, Haley RM, Wechsler ME, Peppas NA, Langer R. Engineering precision nanoparticles for drug delivery. Nature Reviews Drug Discovery. 2020;20(2):101-124.
18. Das KP, J C. Nanoparticles and convergence of artificial intelligence for targeted drug delivery for cancer therapy: Current progress and challenges. Frontiers in Medical Technology. 2023;4.
19. Hossain A, Rayhan MT, Mobarak MH, Rimon MIH, Hossain N, Islam S, et al. Advances and significances of gold nanoparticles in cancer treatment: A comprehensive review. Results in Chemistry. 2024;8:101559.
20. Amina SJ, Guo B. A Review on the Synthesis and Functionalization of Gold Nanoparticles as a Drug Delivery Vehicle. International Journal of Nanomedicine. 2020;Volume 15:9823-9857.
21. Georgeous J, AlSawaftah N, Abuwatfa WH, Husseini GA. Review of Gold Nanoparticles: Synthesis, Properties, Shapes, Cellular Uptake, Targeting, Release Mechanisms and Applications in Drug Delivery and Therapy. Pharmaceutics. 2024;16(10):1332.
22. D'Acunto M, Cioni P, Gabellieri E, Presciuttini G. Exploiting gold nanoparticles for diagnosis and cancer treatments. Nanotechnology. 2021;32(19):192001.
23. Aytar EC, Kahyaoğlu İM, Durmaz A, Karakuş S. Silver/Gold Nanoparticle for Photothermal Therapy of Cancer. Metals in Medicine: Apple Academic Press; 2024. p. 173-204.
24. Rheima AM, Abdul-Rasool AA, Al-Sharify ZT, Zaidan HK, Athair DM, Mohammed SH, et al. Nano bioceramics: Properties, applications, hydroxyapatite, nanohydroxyapatite and

CC BY

drug delivery. Case Studies in Chemical and Environmental Engineering. 2024;10:100869.
25. Localized Phase Separation of Thermoresponsive Polymers Induced by Plasmonic Heating. American Chemical Society (ACS). http://dx.doi.org/10.1021/acs.jpcc.7b07187.s001
26. Zhao Z, Zhang Z, Guo R, Shi W, Zhang Q, Guo Y, et al. Enhanced photo-thermoelectric detection in black silicon with chimney-like texture. Materials Today Communications. 2024;40:109723.
27. Kok HP, Cressman ENK, Ceelen W, Brace CL, Ivkov R, Grüll H, et al. Heating technology for malignant tumors: a review. Int J Hyperthermia. 2020;37(1):711-741.
28. Luan X, Pan Y, Gao Y, Song Y. Recent near-infrared light-activated nanomedicine toward precision cancer therapy. Journal of Materials Chemistry B. 2021;9(35):7076-7099.
29. Qin B, Fu S-j, Xu X-f, Yang J-j, Wang Y, Wang L-n, et al. Far-infrared radiation and its therapeutic parameters: A superior alternative for future regenerative medicine? Pharmacol Res. 2024;208:107349.
30. Yaseen M, Khattak MAK, Humayun M, Usman M, Shah SS, Bibi S, et al. A Review of Supercapacitors: Materials Design, Modification, and Applications. Energies. 2021;14(22):7779.
31. Riaz A, Sarker MR, Saad MHM, Mohamed R. Review on Comparison of Different Energy Storage Technologies Used in Micro-Energy Harvesting, WSNs, Low-Cost Microelectronic Devices: Challenges and Recommendations. Sensors. 2021;21(15):5041.
32. Ali SA, Habib K, Younas M, Rahman S, Das L, Rubbi F, et al. Advancements in Thermal Energy Storage: A Review of Material Innovations and Strategic Approaches for Phase Change Materials. Energy and Fuels. 2024;38(20):19336-19392.
33. Malik S, Muhammad K, Waheed Y. Nanotechnology: A Revolution in Modern Industry. Molecules. 2023;28(2):661.
34. Li J, Li Y, Liu H, Ran F. Nano gold for supercapacitors and batteries. Nano Energy. 2024;128:109839.
35. Mohammed N, Nawar S, Etawy M, Nassar G, Hassabo A. Nanotechnology and its Applications in Industry and Product Design. Journal of Textiles, Coloration and Polymer Science. 2024;0(0):0-0.
36. Sadiq Z, Safiabadi Tali SH, Hajimiri H, Al-Kassawneh M, Jahanshahi-Anbuhi S. Gold Nanoparticles-Based Colorimetric Assays for Environmental Monitoring and Food Safety Evaluation. Crit Rev Anal Chem. 2023;54(7):2209-2244.
37. Mhlanga N, Mphuthi N, Van der Walt H, Nyembe S, Mokhena T, Sikhwivhilu L. Nanostructures and nanoparticles as medical diagnostic imaging contrast agents: A review. Materials Today Chemistry. 2024;40:102233.
38. Esmailzadeh F, Taheri-Ledari R, Salehi MM, Zarei-Shokat S, Ganjali F, Mohammadi A, et al. Bonding states of gold/silver plasmonic nanostructures and sulfur-containing active biological ingredients in biomedical applications: a review. Physical Chemistry Chemical Physics. 2024;26(23):16407-16437.
39. Hsu C-Y, Rheima AM, Mohammed MS, Kadhim MM, Mohammed SH, Abbas FH, et al. Application of Carbon Nanotubes and Graphene-Based Nanoadsorbents in Water Treatment. BioNanoScience. 2023;13(4):1418-1436.
40. Francis DV, Abdalla AK, Mahakham W, Sarmah AK, Ahmed ZFR. Interaction of plants and metal nanoparticles: Exploring its molecular mechanisms for sustainable agriculture and crop improvement. Environ Int. 2024;190:108859.
41. Fathi-karkan S, Easwaran EC, Kharaba Z, Rahdar A, Pandey S. Unlocking Mysteries: The Cutting-Edge Fusion of Nanotechnology and Forensic Science. BioNanoScience. 2024;14(3):3572-3598.
42. Mal S, Chakraborty S, Mahapatra M, Pakeeraiah K, Das S, Paidesetty SK, et al. Tackling breast cancer with gold nanoparticles: twinning synthesis and particle engineering with efficacy. Nanoscale Advances. 2024;6(11):2766-2812.
43. Hou L, Liu X, Ge X, Hu R, Cui Z, Wang N, et al. Designing of anisotropic gradient surfaces for directional liquid transport: Fundamentals, construction, and applications. The Innovation. 2023;4(6):100508.
44. Abdulsada TN, Rheima AM, Al-Rubae'i SHN. Sustainable new biosynthesis of Zero valence gold nanoparticles via Healthy Alchemilla vulgaris L. extract as capping agent. Case Studies in Chemical and Environmental Engineering. 2024;10:100888.
45. Arabi M, Ostovan A, Li J, Wang X, Zhang Z, Choo J, et al. Molecular Imprinting: Green Perspectives and Strategies. Adv Mater. 2021;33(30).
46. Liberty JT, Anil A, Ijimdiya SJ, Kwaji MJ, Ijimdiya RU. Harnessing the potential of nanostructured materials for sustainable development. Nano-Structures and Nano-Objects. 2024;38:101216.

CC BY